

Relationship between the pressure at the casing wall and at the blade tip for a vibrating turbine blade

Osama N. Alshroof, Gareth L. Forbes, Robert B. Randall

The University of New South Wales, School of Mechanical and Manufacturing Engineering,
Kensington, Sydney, NSW 2052, Australia

Abstract

A recent research program has identified the possibility of using the analysis of casing wall pressures in the indirect measurement of gas turbine rotor blade vibration amplitudes [1]. Analytical modelling of the casing wall pressures and reconstruction of rotor blade vibration amplitudes from the analysis of these simulated pressure signals have shown potential advantages over current non-contact rotor blade vibration measurement methods. However, the modelling made some fundamental assumptions about the casing wall pressure. One of the assumptions made was that the pressure at the blade tip is not significantly different from that measured across the clearance gap at the casing wall. This fluid-structure hypothesis is investigated in this paper. Unsteady computational fluid dynamic modelling of the flow conditions around the blade surface, combined with the blade structural motion, is performed numerically, and the distributions of the pressure across the rotor blade tip and casing clearance gap are investigated and reported.

Keywords: blade vibration, casing wall pressure, gas turbine.

Introduction

Blade vibration is unavoidable and inherent in the operation of any gas turbine. The greatest cause of failures in gas turbines is due to the blade faults, reported to be up to 42% [1], such that proper design for these excitation forces is needed. It is therefore paramount that blade vibration can be measured and blade fatigue life estimated.

Gas turbine blade vibration measurement is motivated by the desire to acquire either the blade's forced vibration magnitude and frequency or to estimate the modal parameters of the blade. The impetus for this information is generally driven, respectively, by the need for knowledge of High Cycle Fatigue (HCF) estimates for blade life, or the use of blade modal parameter values for condition monitoring of the blades.

Measurement of blade vibration can be achieved by directly attaching strain gauges to the blade surface, however the attachment of sensors to all blades within the engine is never desirable, and is certainly not practical outside of the design stage. Such are the difficulties of direct measurement of blade vibration, non-contact blade vibration measurement has been sought, with blade tip timing (BTT) methods showing the most promise and receiving research attention since the 1970's. Despite the promise of BTT methods they are still not without limitations or shortcomings four decades after their initial use.

In a recent research project it was proposed that blade vibration would have an effect on the casing wall pressure and casing vibration, and thus measurement of these parameters could be used for monitoring of blade vibration parameters [2]. It was

shown that direct demodulation of simulated internal casing pressure signals could yield the measurement of rotor blade vibration amplitudes [3], and that observation of casing vibration signals could lead to the ability to estimate rotor blade natural frequencies [4]. One assumption made in this previous research was that the pressure at the rotor blade tip is not substantially different from the pressure at the casing wall. This assumption is investigated further in this paper through the use of a three dimensional fluid dynamic modelling of an oscillating rotor blade and investigating the pressure between this rotor blade tip and the casing wall.

Numerous three dimensional computational fluid dynamic studies of gas turbine blades undergoing vibration have been undertaken in the past. One such rigorous numerical study with accompanying experimental results was undertaken by Bell and He [5], where the aerodynamic damping factor for an oscillating blade was investigated along with assessing the effects of various gaps between the blade tip and casing wall surface on this aerodynamic damping factor. However studies such as this are generally interested in the effects of the flow and structural interaction leading to the onset of blade flutter, i.e. the aerodynamic damping factor, along with investigations into the forces which are applied to the rotor blades, being static or dynamic, which could compromise the structural integrity of the turbine disk. Until this recent research study, to the authors' knowledge, this is the first three dimensional CFD study into the change in pressure between the rotor blade tip and casing wall for further use as a blade vibration measurement tool.

Previous computational investigations, without the inclusion of blade vibration, have shown success in using gas turbine pressure signals for determining changes in rotor blade geometry, e.g. blade twist faults [6] and [7]. Both of these studies identified pressure signal fault signatures for different geometric changes and relation of these back to a given fault from the measured pressure from the different geometric conditions relating to the flow from the computational fluid dynamic modelling.

A three dimensional fluid dynamic model of a sector of a rotor blade stage, with the rotor blade forced to vibrate at a given stator passing frequency, will now be developed and pressure changes across the domain from the blade tip to the casing surface will be discussed.

Rotor blade vibration

As has already been stated, vibration of gas turbine blades is an inherent attribute of their use, and is driven by two groups of forces, those being from stochastic processes in the fluid flow and from the periodic traversing of high and low pressure regions from the preceding stator blade row. Rotor blade vibration is then generated from the passing of the stator blade stages. This blade vibration has been enforced on the rotor blade in the following

numerical modelling, forcing the rotor blade section to move normal to the turbine's axis of rotation.

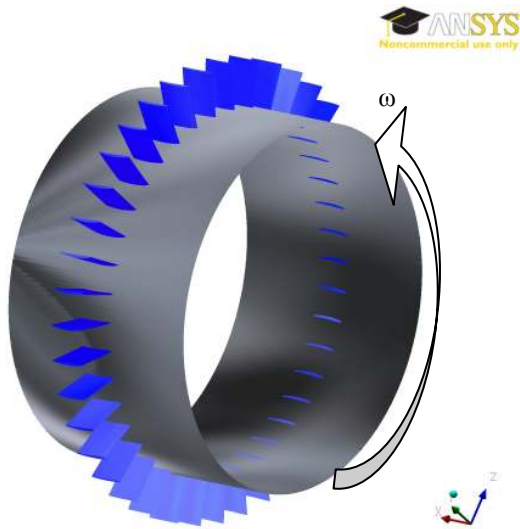


Figure 1: Schematic view of gas turbine stage, presented is the hub and 40 rotor blades. The external casing is not shown.

A three dimensional rotor was modelled as shown in Figure 1, with 40 blades of 50mm length and 50mm chord length mounted on a 200mm diameter hub rotating with angular velocity, ω , of 1000rad.s^{-1} . The number of stator blades for this simulated turbine was set at 32, such that the enforced motion on the rotor blades was given this stator passing frequency of 32000rad.s^{-1} with the maximum blade tip amplitude of 2mm. In order to reduce the computational power needed to solve this problem, a three dimensional wedge, as is shown in Figure 2, was simulated using the following boundary conditions:

Boundary Conditions

Inlet → Inlet velocity= $[237i+ 38j +0k]\text{m.s}^{-1}$, in which i, j and k are the unit vectors for x,y and z coordinates as shown in Figure 2.

Outlet → Average relative static pressure = 0.

Hub → Nonslip wall.

Blade → Nonslip wall with forced vibration added to represent the response to forces from the periodic traversing of high and low pressure regions from the preceding stator blade row. The vibration of the rotor blade is presented as a sinusoidal displacement as a function of time and position in the z direction as follows:

$$\delta = 0.8 \times \sin(32000 t) \times (z - 0.2)^2, \quad (1)$$

in which 32 stator blades are assumed.

The two wedge sides → defined using rotational periodicity.

All the above boundary conditions are rotating at 1000rad.s^{-1} , whereas, the casing surface is defined as a stationary nonslip wall.

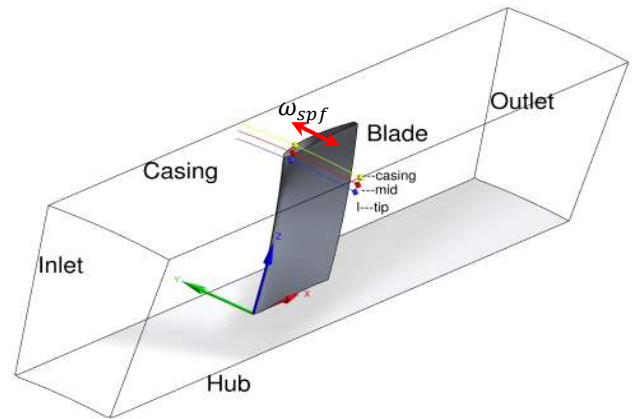


Figure 2 Three dimensional blade model. Also shown are the polylines and points where the pressure distribution is observed.

Solution Method

The problem was solved for incompressible air flow at 25°C with constant properties, by obtaining the steady state velocity fields by using a commercial package, ANSYS CFX-12.1. A transient solver with a second order backward Euler differencing scheme was used for the transient term and SST turbulence model with a high-resolution scheme (between first and second order scheme) was employed for the advection terms in the Navier-Stokes equation. Internal iterations were continued until the mass, momentum and energy residuals had been reduced to 10^{-6} at each time step.

Details of the grid

The mesh has to follow the displacement of the blade, therefore the mesh has to be expanded and compressed. In order to allow this deformation of the mesh, a structured mesh was generated as shown in Figure 3. A hexahedral O-grid is placed around the blade and a normal hexahedral grid filled out the rest of the computational domain as is shown in Figure 3(a). A total of one million mesh elements is used in the discretization.

The body fitted grid was concentrated over the blade and its surrounds so as to adequately resolve the complex flow structures around it.



Figure 3 View of a structured grid at (a) horizontal plane crossing the blade tip and (b) cross section plane located at the blade centre.

Results and discussion

The pressure between the rotor blade tip and the casing surface is interrogated across three polylines, as shown in Figure 2e 2, where the pressure is plotted for three different instances in time being, maximum blade deflection, minimum blade deflection and half of the maximum blade deflection. At three different locations on these polylines the pressure is also plotted across three stator passing periods.

The pressure profile across the width of the rotor blade sector, over the polylines shown in Figure 2, for the three instances in time at the blade tip, midway (across the tip gap) and at the casing surface are shown in Figure 4(a), (b) and (c). Although the magnitude of the pressure distributions in Figure 4 are not the same along the polylines, the pressure distributions are generally of a similar shape, even by comparing it to the average solution (Figure 4(d)). The largest difference between the measurements is at the blade tip; this larger difference is thought to be due to the fact that the blade tip pressure has the highest gradient (stagnation pressure) and also the most complex flow structure. Measurement of the pressure at a slightly offset distance from the blade should show a greater convergence between all of the pressure distributions across the rotor blade sector width.

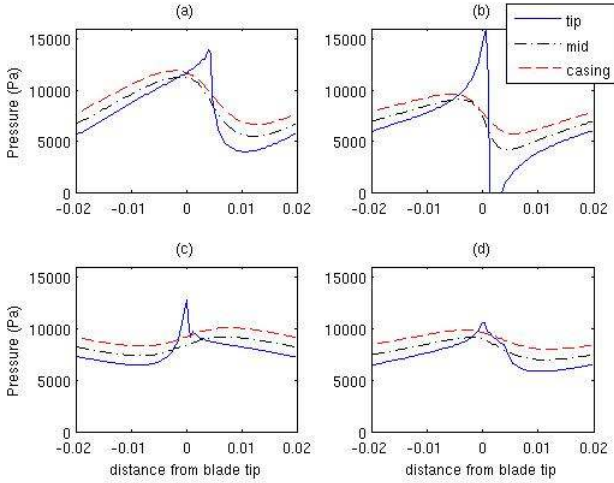


Figure 4 Pressure across the three polylines, as shown in Figure 2, when the blade deflection is (a) at a maximum, (b) at a half of the maximum, (c) at a minimum and (d) time-averaged.

Observation of the pressure distributions across the rotor blade sector show that the pressure distribution is very much dominated by a pressure distribution which spans one period across the rotor blade sector, most notable in Figure 4(a). This could be simulated analytically simply by a combination of sine waves such as:

$$P = \left(\sin(\omega_{bpf}t) - 0.4 \sin(2\omega_{bpf}t) + 1 \right) / 2 \quad (2)$$

The above analytical pressure distribution is shown in Figure 5. It can be seen that this pressure distribution is similar to that in Figure 4.

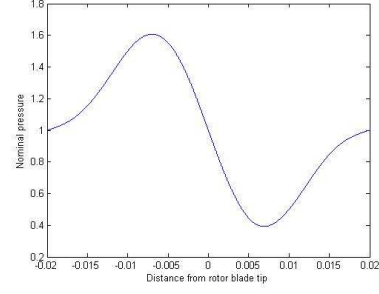


Figure 5 Analytical pressure distribution across blade sector span

As the rotor blade vibrates back and forth, the rotor blade will force this pressure distribution to move back and forth with its motion.

This back and forth motion modulates the rotor blade pressure distribution, such that observation of the pressure distribution will be harmonic when viewed over time.

This harmonic pressure change over time can be seen in Figure 6 and Figure 7. It can be noticed from these figures that the change in pressure contains not only harmonics at the stator passing period, but at higher frequencies, particularly twice the stator passing period (most notable in Figure 7(a) and (b)). This is due to the modulating of the rotor blade sector pressure distribution.

Once again this modulation could be modelled as a simple analytic function, as shown below.

$$P = \left(\sin(\omega_{bpf}t + 0.63 \cos(\omega_{spf}t)) - 0.4 \sin(2\omega_{bpf}t + 1.26 \cos(\omega_{spf}t)) + 1 \right) \quad (3)$$

It can be seen that this function is the same as the function used to simulate the pressure distribution across the rotor blade sector, however the phase is changing at the frequency which the rotor blade is vibrating thus modulating the pressure distribution. This then creates a varying signal with time which contains higher harmonics of the modulating frequency, being higher harmonics of the blade vibration frequency. The similarities between the pressures obtained from the 3D CFD model and the above analytical representation can be seen in Figure 6 and Figure 7.

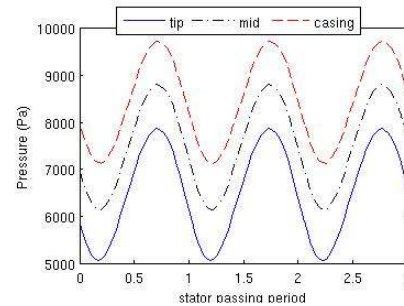


Figure 6 Pressure at the three point locations at the periodic boundary across time, presented in Figure 2.

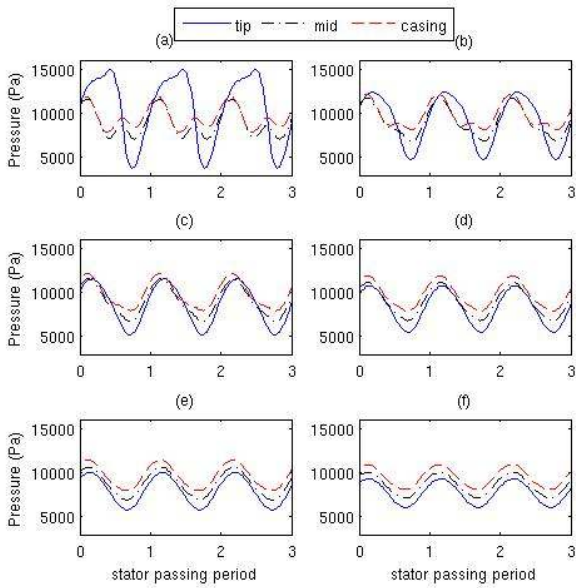


Figure 7 Pressure at the three points located at (a) the blade tip, (b) 10%, (c) 20%, (d) 30% and (f) 35% of the distance from the blade tip to the side of the sector shown in Figure 2.

Pressure contours across the blade tip gap during the blade motion can be seen in Figure 8. Observation of these contours in conjunction with the change in pressure at the monitoring points in Figure 7, it is possible to see that although there is a magnitude difference between where the location of the pressure is measured, being at the blade tip, midway between the tip and the casing or at the casing surface, there is a direct correlation between the pressure across the blade tip gap. Additionally, the pressure also seems to follow the blade's motion such that the blade vibration frequency modulates pressure profile around the

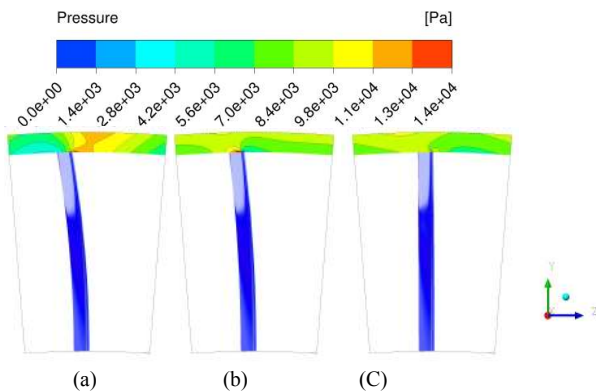


Figure 8 Pressure contours when the blade deflection is (a) at a maximum, (b) at a half of the maximum and (c) at a minimum.

rotor blade resulting in the pressure containing higher harmonics of the stator passing than the rotor blade is vibrating at.

Conclusions

A three dimensional CFD model of a single vibrating blade was constructed. With this model the pressure differences between the vibrating rotor blade tip and the casing surface can be investigated. In this initial stage the rotor blade motion was enforced as well as only a single blade being modelled. This means that no inter-blade pressure interactions are modelled, that is as if there were an equal number of rotor blades as stator blades, as well as the coupled interaction between the blade motion and fluid flow cannot be captured, however it is envisaged that this interaction will have little effect on the ability to conclude how the pressure at the vibrating rotor blade tip and that at the casing wall surface correlate to each other.

It was shown that the pressure between a vibrating blade tip and the casing surface is correlated, and displays the properties which suggest that the pressure profile around the rotor blade follows the pressure profile at the casing. The effects of the size of the gap between the blade tip and the casing surface will be investigated further along with using the results from this numerical model for the phase demodulation of the casing wall pressure in order to estimate the blade tip vibration amplitude in future studies.

Acknowledgments

Grateful acknowledgment is made for the financial assistance given by the Australian Defence Science and Technology Organisation, through the Centre of Expertise in Helicopter Structures and Diagnostics at UNSW.

References

- [1] Meher-Homji, C.B. *Blading vibration and failures in gas turbines part A: blading dynamics & the operating environment*. 1995. Houston, TX, USA: ASME, New York, NY, USA.
- [2] Forbes, G.L., *Non-contact gas turbine blade vibration monitoring using internal pressure and casing response measurements*. 2010, The University of New South Wales: PhD Dissertation. p. 211.
- [3] Forbes, G.L. and R.B. Randall, *Simulation of Gas Turbine blade vibration measurement from unsteady casing wall pressure*, in *Acoustics 2009: Research to Consulting*. 2009, Australian Acoustical Society: Adelaide.
- [4] Forbes, G.L. and R.B. Randall. *Gas Turbine Casing Vibrations under Blade Pressure Excitation*. in *MFPT 2009*. 2009. Dayton, Ohio.
- [5] Bell, D.L., He L. *Three-dimensional unsteady flow for an oscillating turbine blade and the influence of tip leakage*. *Journal of Turbomachinery*, 2000. **122**: p. 93-101.
- [6] Dedoussis, V., K. Mathioudakis, and K.D. Papiliou, *Numerical simulation of blade fault signatures from unsteady wall pressure signals*. *Journal of Engineering for Gas Turbines and Power*, Transactions of the ASME, 1997. **119**: p. 362-369.
- [7] Stamatis, A., N. Aretakis, and K. Mathioudakis. *Blade fault recognition based on signal processing and adaptive fluid dynamic modelling*. 1997. Orlando, FL, USA: ASME, New York, NY, USA.